chemistry proceedings

MDPI

Proceeding Paper

Potential Fluorescent Ligands for Zn-Containing Bacterial Enzymes: In Silico Evaluation, Synthesis and Optical Properties †

Viktoryia Zavalinich [1], Liliya Glinskaya [2], Polina Yakovets [1], Yaroslav Faletrov [1,2,*] and Vladimir Shkumatov [1,2]

[1] Faculty of Chemistry, Belarusian State University, Minsk, Belarus; viktoryiazavalinich@mail.ru (V.Z.); email (P.Y.); biopharm@bsu.by (V.S.)
[2] Research Institute for Physical Chemical Problems, Belarusian State University, Minsk, Belarus; biopharm@bsu.by
* Correspondence: yaroslav82@tut.by
† Presented at the 26th International Electronic Conference on Synthetic Organic Chemistry; Available online: https://ecsoc-26.sciforum.net.

Abstract: Zn-containing proteins play some essential roles in viability and virulence of bacteria, so they consider to be possible molecular new drug targets. Based on literature data about N-acyl-o-phenylenediamine and 2-pycolylamine as warheads of drugs and molecular probes for Zn-bearing enzymes like histone deacetylases we guessed N-(7-nitrobenzofurazan-4-y)-*o*-phenylenediamine (NBD-OPD), 2-pycolyl-(N-(7-nitrobenzofurazan-4-amine)) and ciprofloxacin 2-pycolylamide (CPF-Pic2) as potential fluorescent inhibitors of such enzymes. Molecular docking was performed for estimate affinity of the compounds to a set of bacterial enzymes as well as photochemical and electrochemical properties were in silico calculated using DFT.

Keywords: fluorescent compounds; zinc containing enzymes; DFT; ciprofloxacin; ortho-phenylenediamine; 7-nitrobenzoxadiazole-chloride; molecular docking

Citation: Zavalinich, V.; Glinskaya, L.; Yakovets, P.; Faletrov, Y.; Shkumatov, V. Potential Fluorescent Ligands for Zn-Containing Bacterial Enzymes: In Silico Evaluation, Synthesis and Optical Properties. *Chem. Proc.* **2022**, *4*, x. https://doi.org/10.3390/xxxxx

Academic Editor(s): Julio A. Seijas

Published: 15 November 2022

1. Introduction

Development of fluorescent probes via functionalization of some bioactive molecules (drugs, metabolites) using derivatization with commercially available NBD-chloride is a good abundant decision because NBD has small size (for NBD-NH_2, $C_6N_4O_3H_4$, 17 atoms, two cycles, ~0.5 cubic nm), microenvironment sensitivity, robust synthetic protocols for amines labeling, good fluorescence properties (blue light excitation, more than 50 nm Strokes shift, moderate quantum yields) [1]. Another solution may be fluoroquinolones like ciprofloxacin, which is also active against multiple gram-positive and gram-negative bacteria and mycobacteria. The ability of CPF to fluoresce with blue light and the presence of a fluorine atom together with secondary amine and carboxyl fragments in its structure make it possible to use CPF as a label for its detection in complex environments using approaches based on its fluorescence and ^{19}F-NMR [2–5].

Ortho-phenylenediamine (OPD) can interact with free radicals, it's able to function as a regulator of apoptosis, a substrate for peroxidases and it finds application in studies of oncological, autoimmune and neurodegenerative diseases [6,7]. In addition, N-acyl-OPD derivatives can inhibit histone deacetylases (HDACs) [8,9]. It is known that the closest prototype to NBD-OPD is *N*-NBD-*p*-aminophenol—a fluorogenic substrate of peroxidases [1].

2-picolylamine is used in the synthesis of numerous biologically active compounds. There are a large number of reports in which picolylamine derivatives have been used to

create metal complexes in the property of modifications that reflect the structure and reactivity of metal ion centers in complex biological systems, and also have a wide range of biological activities [10].

Zn-containing proteins play some essential roles in viability and virulence of bacteria, so they consider to be possible molecular new drug targets. Based on literature data about N-acyl-o-phenylenediamine and 2-pycolylamine as warheads of drugs and molecular probes for Zn-bearing enzymes like histone deacetylases we guessed N-(7-nitrobenzofurazan-4-y)-orto-phenylenediamine (NBD-OPD), 2-pycolyl-(N-(7-nitrobenzofurazan-4-amine)) and ciprofloxacin 2-pycolylamide (CPF-Pic2) as potential fluorescent inhibitors of such enzymes. The compounds are in Pubchem database (NBD-Pic2 is AKOS008922865, CPF-Pic2 is a AKOS005560555 homolog, NBD-OPD is SCHEMBL19269457), but, to the best of our knowledge, they are not exhaustively characterized as zinc-bearing bacterial enzymes in silico. For assessment of the biological properties of NBD-OPD, NBD-Pic2 and CPF-Pic2, we conducted a reverse virtual screening based on Autodock Vina [11] using the original assistant program FYTdock with a set of PDB structures of Zn-containing beta-lactamases of bacteria and estimate plasma membrane permeability using PerMM server. Additionally, some optical and electrochemical properties of NBD-OPD were computed using density functional theory to be compared with experimental data.

2. Materials and Methods

OPD, NBD-Cl, 2-picolylamine (Pic2), N-Hydroxysuccinimid (NHS), N,N′-Dicyclohexylcarbodiimide (DCC), tetrahydrofuran (THF), acetonitrile were from Sigma. ciprofloxacin hydrochloride (CPF · HCl) was from Zhejiang LangHua pharmaceutical Co., Ltd. (Linhai, China).

The spectra were recorded on a SOLAR CM-2230 (Belarus) spectrophotometer-spectrofluorimeter. Molecular docking was done using Autodock Vina and FYTdock [12]. Affinity of binding were estimated using Autodock Vina-calculated binding energies (E_{bind}). Additionally, "Zn-match" criterium, meaning a zinc atom proximity to one (+) or two (++) of putative zinc-binding motifs (OPD and 2-picolylamine parts) was invented. Photochemical and electrochemical properties were calculated using a DFT method using the Gaussian 09W and GaussView programs.

3. Results and Discussion

3.1. Docking of CPF-Pic2, NBD-Pic2, NBD-OPD with Zn-Containing Proteins

A part of docking results, showing co-localization of potential zinc-binding diamine motifs of the CPF-Pic2, NBD-Pic2 and NBD-OPD and zinc ions of the bacterial proteins, are summarized in Tables 1, 2 and 3, respectively.

Table 1. E_{bind} values for CPF-Pic2 in silico interactions with structures of Zn^{2+}-containing proteins.

PDB Code	E_{bind}	Organism	Protein	Zn- Match
3HQ2	−10	*Bacillus subtilis*	M32 carboxypeptidase	+
2IGI	−9.1	*Escherichia coli K-12*	Oligoribonuclease	++
2OOG	−8.6	*Staphylococcus aureus*	Phosphodiesterase	+
2NQJ	−8.6	*Escherichia coli*	endonuclease IV E261Q	++
2Z29	−8.2	*Escherichia coli*	Dihydroorotase Thr109Ala	+
1YT3	−8.2	*Escherichia coli*	RNAse D	++
3GRI	−7.8	*Staphylococcus aureus*	Dihydroorotase	+
1Z3A	−7.7	*Escherichia coli*	tRNA adenosine deaminase TadA	+

Table 2. E_{bind} values for CPF-Pic2 in silico interactions with structures of Zn^{2+}-containing proteins.

PDB Code	E_{bind}	Organism	Protein	Zn- Match
2P50	−8.9	*Escherichia coli K-12*	N-acetylglucosamine-6-phosphate deacetylase	+
3ELF	−8.8	*Mycobacterium tuberculosis*	Fructose-bisphosphate aldolase	+
1XAH	−8.3	*Staphylococcus aureus*	3-dehydroquinate synthase	+
4LEF	−8.2	*Escherichia coli K-12*	Phosphotriesterase homology protein	+
2UYV	−8.1	*Escherichia coli*	rhamnulose-1-phosphate aldolase	+
3QBE	−8.0	*Mycobacterium tuberculosis*	3-dehydroquinate synthase	+
4FUA	−8.0	*Escherichia coli*	L-fuculose-1-phosphate aldolase	+
1S7D	−7.9	*Escherichia coli*	Metal-binding Protein yodA	+

Table 3. E_{bind} values for NBD-OPD in silico interactions with structures Zn^{2+}-containing molecules.

PDB Code	E_{bind}	Organism	Protein	Zn- Match
4XND	−9.4	*Escherichia coli*	Isoaspartyl dipeptidase	+
1RRM	−9.3	*Staphylococcus aureus*	3-dehydroquinate synthase	+
2DQM	−8.7	*Staphylococcus aureus*	3-dehydroquinate synthase	+
4UEJ	−8.6	*Escherichia coli K-12*	Homocysteine S-methyltransferase	+
4XMX	−8.5	*Escherichia coli K-12*	Aminopeptidase N	++
1S03	−8.5	*Escherichia coli*	Lactaldehyde reductase	+
2HPT	−8.5	*Escherichia coli K-12*	N-acetylglucosamine-6-phosphate deacetylase	+
5MFS	−8.2	*Staphylococcus aureus*	3-dehydroquinate synthase	++

Thus, the possibility of affine binding (E_{bind} ranges from −10 to −7.9 kcal/mol) to a set of zinc-containing bacterial proteins realizing co-localization of at least one N-atom of putative zinc-binding groups was shown for the small molecules under consideration highlighting ways of their development as possible antibacterial agents. For instance. NBD-OPD amino acids surrounding for calculated complex with 3-dehydroquinate synthase of *Staphylococcus aureus* (PDB 1RRM) was found to be Val164, Cys362, Leu259, His263, His267, His200, His277, Asn151, Asp102, Tyr152, Val153, Thr144, Gly98, Lys162, Asn71, Ser99 and Zn387 ion.

3.2. Evaluation of Membrane Permeability In Silico

To study the biological properties of NBD-OPD, a theoretical assessment of the penetration of the studied substances into the cell by the effectiveness of their passive diffusion through the lipid bilayer was carried out (Table 4). The evaluation was carried out using the PerMM service using default parameters (parameters: pH 7.35, T = 37 °C).

Table 4. Evaluation of the penetration of the studied substances into the cell by the efficiency of their passive diffusion through the lipid bilayer.

	Free Binding Energy	Logarithm of the Permeability Coefficient				
	(DOPC), kcal/mol	(Plasma Membrane)	(BLM)	(BBB)	(CACO2)	PAMPA-DS
NBD-Cl	−9.47	1.27	-	−1.52	−2.48	-
OPD	−2.31	−3.61	−2.14	−3.65	−4.03	−3.20
NBD-OPD	−4.77	−2.71	−1.02	−3.26	−3.74	−2.17
CPF-Pic2	−2.32	-	−5.64	−4.88	−4.92	−6.43
NBD-Pic2	−4.45	−0.58	-	−3.10	−3.63	-

pH = 7.4, T = 298 K; logP values > −4.35 for BBB indicate the ability of the substance to be passively transported through the corresponding membranes.

These results indicate that phospholipid membranes are generally permeable to NBD-OPD and NBD-Pic2, but CPF-Pic2 seems not to be good for passive diffusion through a phospholipid membrane.

3.3. Results of Quantum Chemical Calculations for NBD-OPD Structure

The complete optimization of the geometry of the studied compounds was carried out by the DFT method using the B3LYP functional and the polarization basis set 6–31 g + (d, p). The calculated geometric parameters related to the bonds in the ground (S0) and excited (S1) states tabulated in Table 5. The calculated value of the short contact S0 O---H was 2.39 Å (versus 2.37 Å, S1 in NBD-Cl and 2.41 Å, S1 in NBD-OPD), which is significantly less than the sum of van der Waals radii (2.72 Å). The short contact N---O (decreases in the excited state) is significantly less than the sum of the van der Waals radii (3.07 Å). In addition, the contact D5 N---H (smaller than the sum of the van der Waals radii (2.75 Å)) may vary. Other (N---H) contacts are sensitive to amino-substituted groups. As a result, these contacts were identified as an important driving force for the stabilization of the studied coplanar molecular structures. The main difference in the ground and excited state is the change in the torsion angle ϕ and the dipole moment. It was found that the dipole moment of the singlet excited state is less than the dipole moment of the ground state. It is important to note that the lengths of C---NO_2 bonds decrease by 0.3 Å during excitation due to the effect of the electron acceptor nitro group.

Table 5. Calculated atom distances D1, O(-NO_2)---H(benzene ring), D2, N(oxadiazole)---O(-NO_2) of NBD fragment as well as and D3 and D4, N(-NH_2)---H(benzene), involved in the formation of intramolecular contacts in the ground (S0) and excited (S1) states of the studied compounds in acetonitrile. The values shown below and highlighted in bold are obtained for S1.

	Intramolecular Short Contacts (Å)					**Covalent Bonds (Å)**		**Dihedral Angle**	**Dipole Moment (D)**
	D1 O···H	**D2 N···O**	**D3 N···H**	**D4 N···H**	**D5 N···H**	**dC-N (1)**	**dC-N (2)**	**ϕ (°)**	
NBD-Cl	2.391 **2.37**	2.797 **2.756**	-	-	-	1.452 **1.428**	-	-	7.235 **7.980**
OPD	-	-	2.656 **2.652**	2.649 **2.657**	-	-	-	-	3.385 **3.305**
NBD-OPD	2.393 **2.406**	2.807 **2.782**	2.679 **2.719**	2.670 **2.657**	2.513 **2.596**	1.420 **1.390**	1.349 **1.417**	128.63 **94.778**	14.55 **12.403**

The calculation method within the framework of the theory of DFT//B3LYP/6-31+ g(d,p) in the model environment of acetonitrile provides good accuracy of predictions of optical properties. And the same approach can be used to predict the general descriptors of reactivity, including chemical potential (μ), chemical resistance (n) and electrophilicity index (W). Also, the energies of the ground (−26,178.4 eV) and excited S1 (−26,176.7 eV) states, the energy levels of the highest occupied (HOMO) and lower free (LUMO) molecular orbitals were calculated for NBD-OPD (Table 6); The electrophilicity values are calculated according to Equation (3) based on μ and n, which can be estimated using Equations (1) and (2) (Table 6).

$$\mu \approx \frac{1}{2}(\varepsilon_{HOMO} + \varepsilon_{LUMO}) \quad (1)$$

$$\eta \approx \frac{1}{2}(\varepsilon_{LUMO} - \varepsilon_{HOMO}) \quad (2)$$

$$w = \frac{\mu^2}{2\eta} \quad (3)$$

Table 6. Calculated HOMO and LUMO energy levels and extracted chemical reactivity descriptors for the studied compounds using DFT//B3LYP/6-31+ g(d,p) in acetonitrile.

Compound	Energy Levels		Chemical Reactivity Descriptors		
	εHOMO (eV)	εLUMO (eV)	μ (eV)	η (eV)	W (eV)
NBD-Cl	−7.621	−3.916	−5.769	1.853	8.981
OPD	−5.469	−0.2584	−2.864	2.605	1.574
NBD-OPD	−6.046	−3.355	−4.701	1.346	8.211

4-amino substituted NBD is recognized among to the broad family of intra-molecular charge transfer (ICT) complexes. The ICT characteristics are identified by the presence of both electron donor and withdrawing acceptor substituent moieties within the same molecule. Thus, the photoinitiated electron transfer from the donor to the acceptor sites yields two kinds positive and negative charges within separated functional parts of the molecule. Herein, we have extracted the atomic Mulliken charges from both ground- and excited-geometry structures. The results are illustrated in Figures 1 and 2. In fact, the 4-amino substituted NBD belongs to the broad family of ICT molecules, with the amino group acting as an electron donor upon photo-excitation, and the nitro (NO2) group as an electron acceptor.

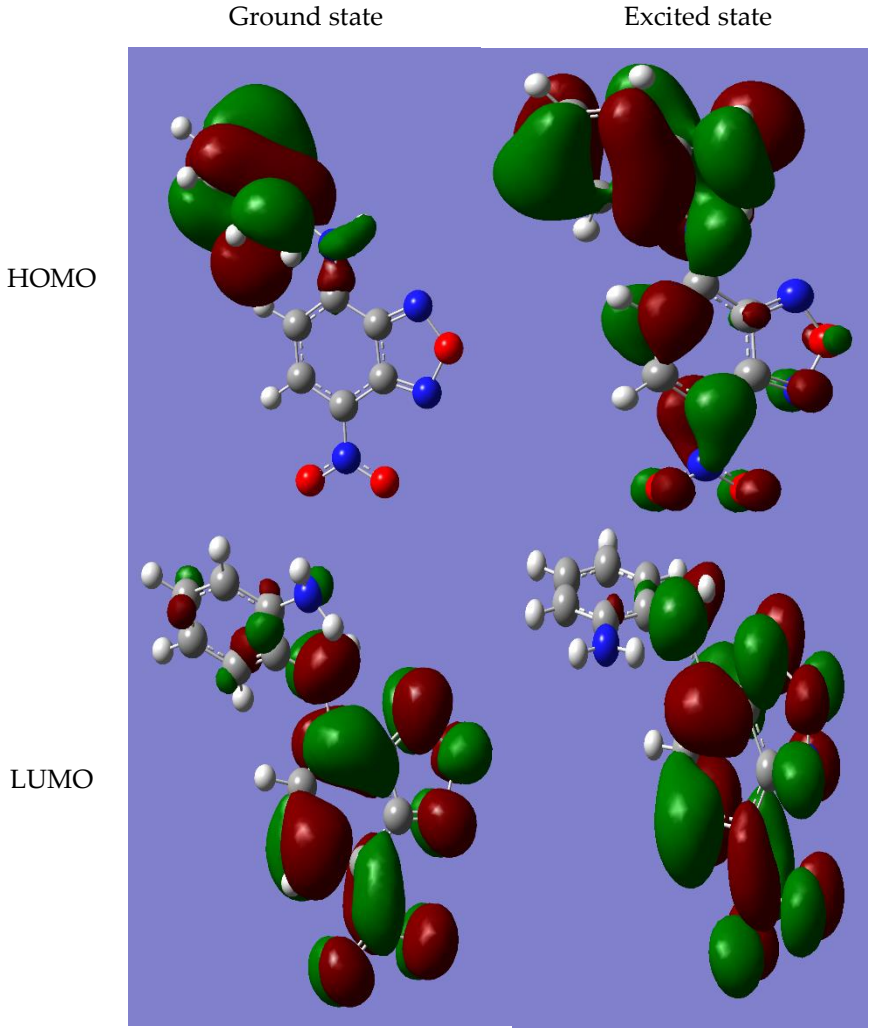

Figure 1. Boundary molecular orbitals (MOS) obtained in the ground (S0) and excited (S1) states of the optimized geometries of NBD-OPD.

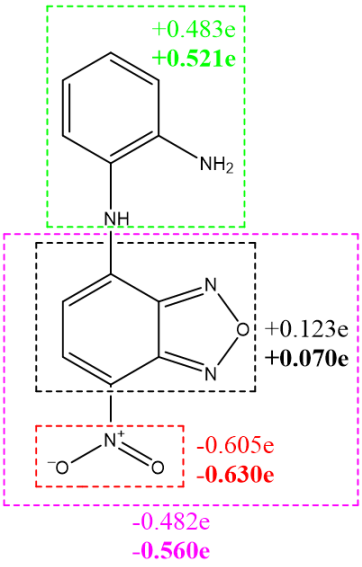

Figure 2. The Mulliken charge distribution of the ground and excited (values highlighted in bold) states of the optimized structures of NBD-OPD.

3.4. Synthesis and Solvatoshromic Properties of NBD-OPD and NBD-Pic2

Synthesis of NBD-OPD and NBD-Pic2 were done using known methods as described [13]. Purity were evaluated using TLC. For NBD-Pic2 Rf is 0.3 in the system benzene:acetonitrile in a ratio of 17:3. For NBD-OPD Rf is 0.75 in the system benzene:ethanol in a ratio of 10:1.

The light absorption and fluorescence emission spectra of the resulting compound were recorded in media with various solvents, and these spectra were also modeled in an acetonitrile medium using density functional theory (DFT) (Figure 3). Absorption streaks are known for NBD-Cl (262 nm and 340 nm) and OPD (297 nm), for NBD-OPD, which is formed during the nucleophilic aromatic substitution reaction, a new optical streak in the range of 467–477 nm is observed, due to intramolecular charge transfer between electron-donating amino- and electron-acceptor nitro- and oxadiazole groups. The middle streak at a wavelength of about 340 nm refers to the electronic transition $\pi \rightarrow \pi^*$. It is important to note that the maxima of the charge transfer bands in these systems are detected in the visible region of the spectra. Thus, the excitation corresponding to the lowest energy band of these compounds was used to investigate the excitation process from the ground (S0) to the first excited state (S1). The emission spectra of NBD-OPD show that the compound has poor fluorescence.

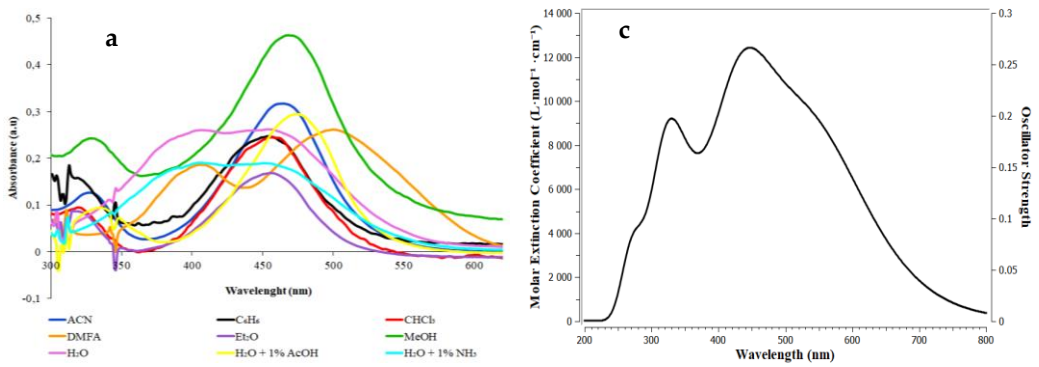

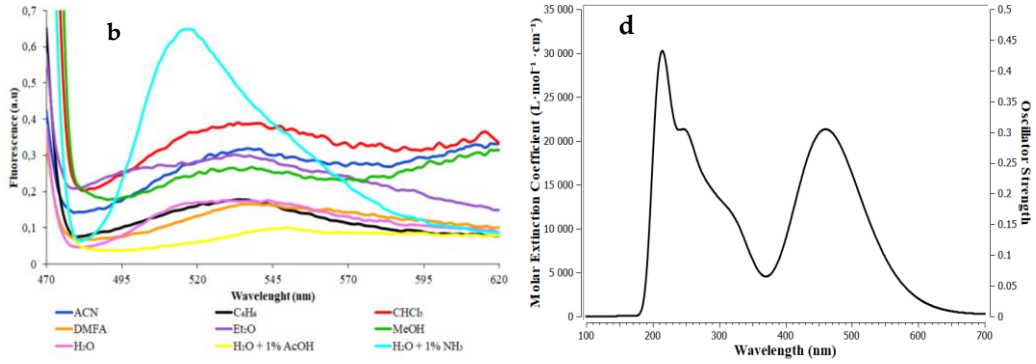

Figure 3. (**a**,**b**): absorption and emission spectra of NBD-OPD, respectively; (**c**,**d**): absorption and emission spectra of NBD-OPD simulated in the framework of DFT in an acetonitrile medium, showing a good level of correlation of experimental and calculated results for absorption spectra.

We also conducted a study of the solvatochromic effect for NBD-Pic2. The spectral region 250–620 nm was studied by spectrophotometry and spectrofluorimetry on a SolarCM2203 instrument at compound concentrations of about 4.0×10^{-5} mol L^{-1} in solvents of different polarity. Emission spectra were recorded using excitation at 460 nm (NBD).

The spectra show a red solvatochromic shift of the absorption maximum by about 15 nm with increasing solvent polarity, with absorption maxima ranging from 430 (petroleum ether) to 475 nm (water) (Figure 4a). These bathochromic shifts confirm the ability of the probe to change the absorption wavelength as the polarity of the environment increases due to interaction with solvent molecules. In an aqueous solution, a significant decrease in the emission intensity was observed compared to organic solvents (Figure 4b).

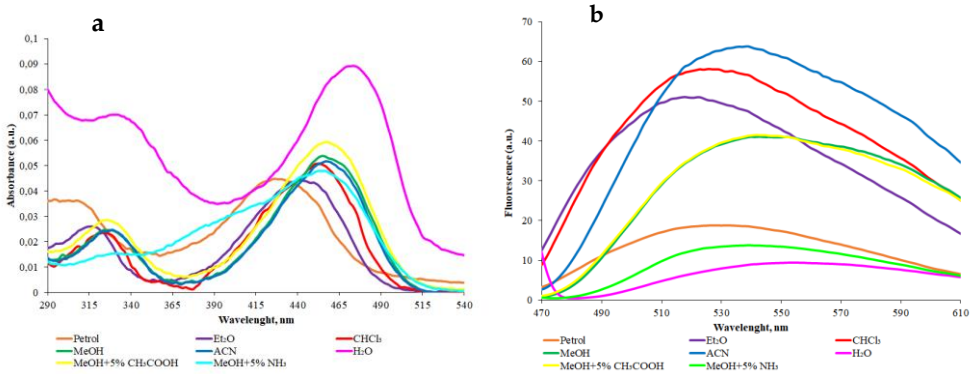

Figure 4. (**a**,**b**): absorption and emission spectra of NBD-Pic2, respectively.

4. Conclusions

Tree structures with putative zinc-binding groups (ZBG), namely, 7-nitrobenzofurazan-4-yl (NBD) 2-picolylamine (NBD-Pic2, AKOS008922865), ciprofloxacin 2-picolylcarboxamide (CPF-Pic2, AKOS005560555 homolog) and N-NBD-ortho-phenylenediamine (NBD-OPD, SCHEMBL19269457) were evaluated by the docking-based virtual screening approach performed using Autodock Vina and FYTdock for effective organization and results analysis. It was found that NBD-OPD can be bound affinely locating its ZBG close to Zn^{2+} of bacterial proteins, namely, Escherichia coli K-12 Aminopeptidase N (PDB 4XMX), Staphylococcus aureus 3-dehydroquinate synthase (1RRM) and few others structures. NBD-Pic2 was found to be able to bind similarly with, e.g., Mycobacterium tuberculosis fructose-bisphosphate aldolase (PDB 3ELF) as well as CPF-Pic2 was found to have similar binding mode with respect to *Escherichia coli* oligoribonuclease (PDB 2IGI). In silico

evaluation of mammalian phospholipid membrane permeation allowed to find bad permeability for CPF-Pic2. Additiona DFT calculations, synthesis of the collored NBD derivatives and solvatochromic tests alllowed to have deeper veiw on perspectives of possible usage of the structures as initial points for design of antibacterials or molecular probes.

Acknowledgments: The work was supported governmental grants of republic of Belarus № of registration 20210560, № 20220695 and a personal grant of Wargaming.net to V.Z.

Conflicts of Interest:

References

1. Wang, C.; Yan, S.; Huang, R.; Feng, S.; Fu, B.; Weng, X.; Zhou, X. A turn-on fluorescent probe for detection of tyrosinase activity. *J. Anal.* **2013**, *138*, 2825–2828.
2. Zimmermann, E.S.; Torres, B.G.; Dalla Costa, T. Validation of a sensitive HPLC/fluorescence method for assessment of ciprofloxacin levels in plasma and prostate microdialysate samples from rats. *Biomed. Chromatogr.* **2016**, *30*, 330.
3. Faletrov, Y.V.; Glinskaya, L.I.; Khoretsky, M.S.; Panada, Y.V.; Frolova, N.S.; Shkumatov, V.M. Synthesis of triazole-containing ciprofloxacin conjugate and its in silico test as a cytochrome P450 ligand. *J. Belarusian State Univ. Chem.* **2021**, *1*, 21.
4. Gee, C.T.; Arntson, K.E.; Urick, A.K.; Mishra, N.K.; Hawk, L.M.; Wisniewski, A.J.; Pomerantz, W.C. Protein-observed ^{19}F-NMR for fragment screening, affinity quantification and druggability assessment. *Nat. Protoc.* **2016**, *11*, 1414.
5. Xu, Z.Y.; Wu, Z.Y.; Tan, H.Y.; Yan, J.W.; Liu, X.L.; Li, J.Y.; Xu, Z.Y.; Dong, C.Z.; Zhang, L. Piperazine-tuned NBD-based colorimetric and fluorescent turnoff probes for hydrogen sulfide. *R. Soc. Chem.* **2018**, *1*, 1–6.
6. Hu, W.-C.; Pang, J. Ultrasensitive Detection of Bacteria Using a 2D MOF Nanozyme-Amplified Electrochemical Detector. *J. Anal. Chem.* **2021**, *93*, 8544–8552.
7. Loginova, N.V.; Koval'chuk, T.V. Redox-active metal (II) complexes of sterically hindered phenolic ligands: Antibacterial activity and reduction of cytochrome c. Part II. Metal (II) complexes of o-diphenol derivatives of thioglycolic acid. *J. Polyhedron* **2011**, *30*, 2581–2591.
8. Lauffer, B.E.L.; Mintzer, R. Histone deacetylase (HDAC) inhibitor kinetic rate constants correlate with cellular histone acetylation but not transcription and cell viability. *J. Biol. Chem.* **2013**, *288*, 26926–26943.
9. Liu, C.; Zhao, C.; Dong, H.; Xu, Q.; Chou, C.J.; Zhang, Y. Synthesis and biological study of class I selective HDAC inhibitors with NO releasing activity. *Bioorg. Chem.* **2020**, *104*, 2–8.
10. Rudbari, H.A.; Kordestani, N.; Cuevas-Vicario, J.V.; Zhou, M.; Efferth, T.; Correia, I.; Schirmeister, T.; Barthels, F.; Enamullah, M.; Fernandes, A.R.; et al. Investigation of the influence of chirality and halogen atoms on the anticancer activity of enantiopure palladium(II) complexes derived from chiral amino-alcohol Schiff bases and 2-picolylamine. *New J. Chem.* **2022**, *46*, 6470.
11. Trott, O.; Olson, A.J. AutoDock Vina: Improving the speed and accuracy of docking with a new scoring function, efficient optimization, and multithreading. *J. Comp. Chem.* **2010**, *31*, 455.
12. Faletrov, Y.V.; Staravoitava, V.A.; Dudko, A.R.; Shkumatov, V.M. Application of docking-based inverse high throughput virtual screening to found phytochemical covalent inhibitors of SARS-CoV-2 main protease, NSP12 and NSP16. *Res. Sq.* **2022**, *1*, 1–20.
13. Bem, M.; Badea, F.; Draghici, C.; Caproiu, M.T.; Vasilescu, M.; Voicescu, M.; Beteringhe, A.; Caragheorgheopol, A.; Maganu, M.; Constantinescu, T.; et al. Synthesis and fluorescent properties of new derivatives of 4-amino-7-nitrobenzofurazan. *ARKIVOC* **2007**, *xiii*, 87–104.
14. Faletrov, Y.V.; Karpushenkova, V.S. Interaction of nitrobenzoxadiazole derivatives of piperazine and aniline with bovine serum albumine in silico and in vitro. *J. Belarusian State Univ. Chem.* **2021**, 25–35.